
Polishing PMMA and Other Optical Polymers with Magnetorheological Finishing

Introduction

Polymer optics are typically manufactured by injection molding (thermoplastics, high volume, economical), compression molding (thermosets, higher precision, and larger sizes), or diamond turning. Once formed by these techniques, polymer components are used “as manufactured,” usually without further cold working to improve surface finish or figure. This is because optical polymers are soft and possess high linear expansion coefficients and poor thermal conductivities.¹ Attempts to improve surface finish and figure using conventional grinding and polishing processes usually result in scratching, the embedding of abrasive particles, the formation of “orange peel,”² and degradation to surface figure. There are circumstances when it would be desirable to perform a classical polishing operation on a polymer surface. In some instances it is desirable to drive rms surface roughness values below 2 to 4 nm in preparation for deposition of a coating. In other applications, reduced surface form errors are required. It is advantageous to eliminate the unwanted flare from diamond-turning marks on polymer optics in order to test prototype imaging system designs.

Magnetorheological finishing (MRF) is a new polishing process that was invented and developed by an international group of collaborators at the Center for Optics Manufacturing (COM) in the mid-1990s³ and commercialized by QED Technologies, Inc. in 1997.⁴ MRF is based on a magnetorheological (MR) fluid consisting of nonmagnetic polishing abrasives (typically CeO₂ or nanodiamonds⁵) and magnetic carbonyl iron (CI) particles in water or other carriers. With the appropriate MR fluid, MRF has successfully polished a variety of materials to subnanometer rms surface-roughness levels with peak-to-valley (p-v) form accuracies to better than 20 nm. Polished materials include optical glasses (fused silica, BK7, SF6, LaK9), hard crystals and polycrystalline glass-ceramics (silicon,⁶ sapphire,⁷ Zerodur, and Nd: YLF⁸), soft UV and IR materials (CaF₂,⁹ AMTIR-1,¹⁰ polycrystalline ZnS,¹⁰ and soft phosphate laser glass), and soft, water-soluble potassium dihydrogen phosphate (KDP) frequency-conversion crystals.¹¹

A normal force of the order of 0.01 N between the abrasive particle and the part is the key to removal in most classical polishing processes. In MRF, however, there is almost no normal load.¹² Figure 96.38 shows a schematic of a part being placed into a ribbon of MR fluid. Shear stresses in the converging gap and the lateral motion of polishing abrasives across the part surface cause material removal without subsurface damage, leaving extremely clean, pit- and scratch-free surfaces. This has been shown to minimize the embedding of polishing powders,¹³ and it suggests that MRF is an excellent candidate for polishing polymer optics.

The following sections describe our work to polish optical polymers with MRF. Materials of interest include polymethylmethacrylate (PMMA), cyclic olefin polymer (COP), polycarbonate (PC), and polystyrene (PS). Goals for removal rate, surface form error reduction, and surface microroughness reduction are established; materials of interest and forms of supply are identified; metrology instrumentation and testing protocols are given; and MRF platforms are briefly reviewed. No single MR fluid was found to be entirely successful in smoothing all polymers tested; therefore, results are presented for several MR fluid and polymer combinations. Variations in the type of nonmagnetic polishing abrasive were seen to make a difference in the ability to polish. Surface degradation observed for some polymers was overcome by changing the polishing abrasive in the MR fluid. Encouraging results for PMMA are described in detail. It was possible to demonstrate both surface figure correction and smoothing in the same processing sequence. Diamond-turning marks were eliminated. Finally, the thermalization issue in cold working of optical polymers is discussed within the context of experiments that encountered long metrology cycle times and long-term figure instability.

Methodology

1. Polymer Materials and Forms of Supply

Polymers used in this work and their trade names are identified in Table 96.I, where they are rank ordered by

hardness.¹⁴ Forms of supply consisted of molded plano coupons, used as received, and/or rod stock that was subsequently diamond turned into plano pucks prior to use. Initial roughness values for the surfaces of the molded coupons (areal, $250\ \mu\text{m}$ by $350\ \mu\text{m}$; see **Metrology and Testing Protocols**, p. 241, for metrology protocols) were in the range of 300 nm to 1600 nm p-v and 2 nm to 11 nm rms. Molded-coupon surfaces were not sufficiently flat to allow for interferometric form metrology. Initial roughness values for the surfaces of the diamond-turned pucks were in the range of 50 nm to 1500 nm p-v and 4 nm to 17 nm rms. Flatness values for the diamond-turned pucks were less than $5\ \mu\text{m}$ p-v (95% aperture).

2. MRF Machine Platforms and Screening Experiments

Three MRF platforms were used to carry out experiments. The principal author and her lab partner¹⁸ conducted an initial screening experiment in late 2001 on the permanent magnet machine (PMM),¹⁹ a test bed primarily intended for undergraduate training in the basics of MRF. The goal of this work was to examine only the smoothing capability of nanodiamond abrasives contained in one of the commercial MR fluids, although the exact MR fluid formulation used was experimental and not entirely aqueous-based. A 60-s-duration circle was polished into a molded coupon at a part rotation rate of 200 rpm. Results for the four polymers listed in Table 96.I were

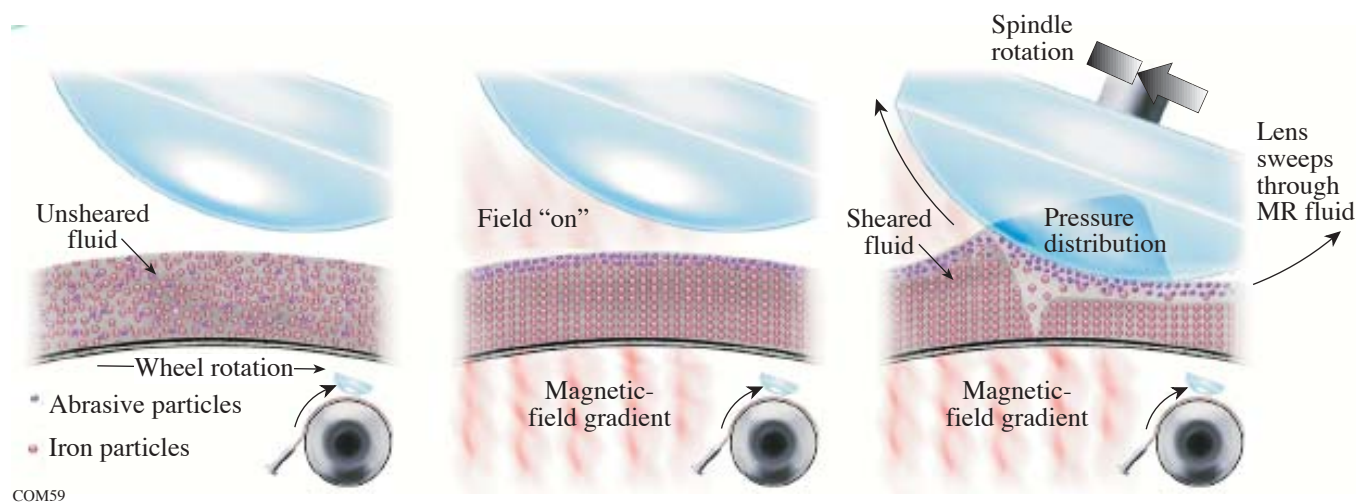


Figure 96.38

Polishing with MRF. (a) The rotating wheel carries the MR fluid ribbon under the part. (b) With the application of a magnetic field, the carbonyl iron particles form an organized structure and are pulled down toward the increasing gradient in magnetic field. Water and the polishing abrasive remain at the surface of the ribbon. (c) A converging gap is formed by placing the part into the ribbon. Solid cores of magnetic fluid form before and under the part, forcing the abrasive particles into a thin, $\sim 150\text{-}\mu\text{m}$ channel with high velocity. Shear against the part surface causes material removal with negligible normal force.

Table 96.I: Polymer materials, forms of supply, and sizes.

Polymer	Trade Name	Rockwell (M hardness)	Form	Size (mm diameter \times thickness)	Ref.
PMMA	Acrylic	97	Molded coupons	50×2.5	(15)
			Rod stock for pucks	48×25	(16)
			Rod stock for pucks	$38 \times \sim 8$	(17)
PS	Dow Styrene	90	Molded coupons	50×2.5	(15)
COP	Zeonex	89	Molded coupons	50×2.5	(15)
			Rod stock for pucks	$75 \times 25, 50 \times 8$	(16)
PC	Lexan	70	Molded coupons	50×2.5	(15)

encouraging, showing that rms roughness levels of the order of 1 to 3 nm could be achieved.

In early 2002, a series of experiments were conducted on diamond-turned PMMA and COP pucks using an MRF research platform called the spot-taking machine (STM). As previously described,¹¹ the STM is used to take spots on stationary part surfaces; it cannot be used to polish out a surface. The STM is intended for evaluating long-term MR fluid stability, material-removal rates for new MR fluids and/or new materials, spot shapes, and in-spot roughness. (In-spot roughness is higher than that achieved with polishing on a rotating part.) Results for experimental MR fluids revealed differences between the two materials under identical test conditions. Peak removal rates as large as 10 $\mu\text{m}/\text{min}$ and 20 $\mu\text{m}/\text{min}$ were obtained for COP and PMMA, respectively. These results did not correlate with material hardness. In-spot roughness values for both materials were reduced to 3 nm rms (COP) and 6 nm rms (PMMA). Diamond-turning marks were eliminated inside a spot taken on the COP part.²⁰

Most of the experiments reported in this article were conducted during 2002 and 2003 on the QED Technologies Q22Y²¹ machine used in rotational mode and programmed for uniform removal of material and/or for figure correction. Commercial CeO₂-based and nanodiamond-based MR fluids, as well as a number of experimental MR fluid formulations, were used under normal and “gentle” operating conditions. Experiments were performed with either the standard 150-mm-diam wheel installed in the machine or a smaller 50-mm-diam wheel. Wheel size affected spot size and removal rate, but it was assumed not to be an issue in evaluating smoothing of surfaces for different abrasives. Parts were mounted in the Q22Y work spindle using vacuum chucks and adapters provided with the machine. This facilitated easy removal of parts for in-process and post-process metrology, without the need for blocking and deblocking with waxes.

3. Metrology and Testing Protocols

The purpose of the work in 2002 and 2003 was to evaluate the potential of using MRF to process optical polymers. Specific objectives were to establish material-removal rates and to demonstrate reductions in surface roughness (white-light interference microscopy²²) and in surface form errors (phase-shifting laser interferometry²³). Metrology was performed in a room ($T = 68 \pm 1^\circ\text{F}$) separated from the Q22Y, which was located on the shop floor ($T = 71 \pm 1^\circ\text{F}$). Spotting was done on designated parts to determine removal rates for a given MR fluid on each polymer. For this, the Q22Y was automatically

programmed to take a series of four individual spots on the part surface. The spots were then evaluated interferometrically and reprocessed by the Q22Y software to calculate average peak removal rates.

Surface roughness was evaluated in either of two ways: Polymer coupons not previously spotted were rotated and polished with uniform removal runs. Five sites, randomly distributed over the part surface, were sampled after polishing for rms roughness. Standard instrument settings²² were employed. For some experiments with ZrO₂, the data were processed with an 80- μm high-pass filter. Diamond-turned pucks were evaluated for roughness in the same manner after 0.5- μm uniform removal runs, and/or after figure correction runs based upon interferometrically determined surface form error maps and removal spot data. Single-surface polishing experiments and one experiment to polish out both sides of a puck were performed.

Several adjustments were made in the metrology lab as a result of mounting and thermalization issues that were encountered. Metal sample-mounting clamps in the interferometer were covered with pads to broaden and reduce zones of high contact pressure on the part barrel. Thermal equilibration of a puck was performed each time it was returned to the metrology lab for testing by covering it with lens tissue and placing it between copper plates for 30 min.

4. Nonmagnetic Polishing Abrasives

Two magnetorheological (MR) fluids are currently in widespread industrial use: One composition consists of micron-sized CeO₂ powder in an aqueous suspension of magnetic carbonyl iron (CI) powder, which has been found appropriate for almost all soft and hard optical glasses and low expansion glass-ceramics. Preparation of this standard MR fluid and its performance have been described previously.²⁴ The second composition uses nanodiamond powder as the polishing abrasive, which is appropriate for calcium fluoride, IR glasses, hard single crystals like silicon and sapphire, and very hard polycrystalline ceramics^{5,11,24} like silicon carbide. Both of these MR fluids were evaluated in this work, even though the abrasives in them are not commonly used for polishing polymers. Considerations leading to a choice of alternative polishing abrasives²⁵ are complex. Not only do the hardness and chemistry of the abrasive grains need to be appropriate to soft polymers, but the type of abrasive (e.g., crystal structure, purity, median size, friability, and surface chemistry) can appreciably affect MR fluid rheology and polishing efficiency.

It has been documented that MR fluid properties in the circulation system of an MRF machine remain constant over a 12-h work day to better than $\pm 1\%$ with either of the standard mixtures, resulting in removal rates that are constant to the same level.²⁶ Alternative abrasives must be capable of forming stable suspensions at high solids concentrations without agglomeration and with good redispersibility. Due to the high concentration and high density (e.g., 7.5 g/cm^3) of CI particles, the MR fluid must be designed to also protect against sedimentation (both static and dynamic) and corrosion. MR fluid pH levels must be kept alkaline when developing new polishing abrasive formulations, again in order to prevent sedimentation and corrosion. A serious reduction in the corrosion resistance was documented for an MR fluid made with a commercial cerium oxide powder that had been milled with an acid during manufacture.²⁷ Another consideration is the potential for abrasive milling by the CI particles, which are known to be harder than most polishing abrasives.²⁸ If this occurs at all, rapid attrition of abrasive median particle size might be preferred to attrition that occurs over a long time period. That said, it has been possible to develop and examine stable aqueous-based MR fluids containing a wide variety of metal oxide polishing abrasives.

All abrasives used in this work were obtained from commercial sources as dry powders, except for the second CeO_2 sample, which was provided as a suspension. Descriptive information for each abrasive is given in Table 96.II without any specific commercial product designations. Use of SnO_2 ,²⁹ ZrO_2 ,³⁰ Al_2O_3 ,^{29,31} and SiO_2 ³¹ was motivated by the existence of these as commercial formulations intended specifically for conventional polishing of polymers. Particle size and the availability of abrasive composition data from the vendor were also important considerations. As shown in the table, many agglomerated micron-size powders were broken down with time into smaller submicron aggregates³² as a result of milling by the MR fluid. This was not the case for the TiO_2 sample, which appeared to be strongly aggregated.

Results

1. Peak Removal Rates and rms Roughness

The forms of supply limited the experiments that could be conducted. Because of their poor surface form quality, coupons of PS and PC were polished with uniform runs, removing an indeterminate amount of material, to yield roughness data. [No spots could be taken on these parts to interferometrically determine removal rates, and therefore spot data from PMMA

Table 96.II: Abrasive particles incorporated into MR fluids for polishing polymers.

Dry abrasive	Purity ^(b)	pH in DI water	Primary particle size ^{(b),33}	Median size ^(c)	Comments
CeO_2 ^(a)	>95% rare earths	7.5	N/A	$1.6 \mu\text{m}$	Milling in MRF machine ^(d) increased vol % of particles < $0.6 \mu\text{m}$ from 3 (3 h) to 15 (48 h); size distribution unchanged for next 10 days
CeO_2 (solution)	91%	N/A	40 nm	96 nm	^(b) Provided as 20.9-wt% solids in pH7.4 solution; size distribution unchanged after milling in MRF machine ^(d) for 7 days
Diamond ^(a)	with graphite	2.5	4 nm	$1.4 \mu\text{m}$	Milling in MRF machine ^(e) increased vol % of particles < $0.6 \mu\text{m}$ from 0.5 to 21 in 7 days
SnO_2	99%	4.7	N/A	370 nm	Large agglomerates broken up with intensive sonication
ZrO_2	98%	7.5	200 nm	$1.8 \mu\text{m}$	Milling in MRF machine ^(d) increased vol % of particles <300 nm from 2 to 11 (4 days) to 72 (11 days)
Al_2O_3	99% γ phase	4.7	33 nm	93 nm	Milling in MRF machine ^(e) increased vol % of particles <225 nm from 0 to 75 in 24 h
TiO_2	99.5% rutile	10.2	$10 \times 40 \text{ nm}$ needles	$2.8 \mu\text{m}$	Milling in MRF machine ^(d) increased vol % of particles < $1.0 \mu\text{m}$ from 2 to 8 in 14 days; aggregates remained
SiO_2	99.8%	4.7	40 nm	N/A	^(b) Amorphous, fumed, crystalline-free, hydrophilic
^(a) Standard MR fluid constituent; ^(b) information supplied by vendor; ^(c) powder dispersed in DI water with a surfactant and intensively sonicated prior to sizing; ³³ ^(d) peristaltic pump system on Q22Y—less aggressive; ^(e) centrifugal pump system on STM—more aggressive.					

was used as input to the machine for performing (estimated) 0.5- μm uniform removal runs.] Spots were taken on diamond-turned pucks of PMMA and COP, thus enabling (precise) 0.5- μm uniform removal runs. Roughness data were obtained from these or from figure correction runs.

Table 96.III gives results for peak removal rate and lowest achieved rms roughness for the four polymers tested. Results are displayed separately for data obtained on diamond-turned pucks and coupons. Selected observations for each polymer are given as follows:

PMMA: Peak removal rates for most abrasives were between 4 $\mu\text{m}/\text{min}$ and 6 $\mu\text{m}/\text{min}$, showing relatively little sensitivity to CI concentration. The higher rates for CeO_2 (solution), TiO_2 , and SiO_2 were obtained with the gentlest machine-

processing conditions (lower magnetic field strength and smaller wheel rpm) and were judged to be too aggressive for use. Removal rates of about 4 $\mu\text{m}/\text{min}$ are entirely adequate for polishing PMMA. For example, using the standard wheel on the Q22Y under normal operating conditions with either the standard CeO_2 -based or nanodiamond-based MR fluid, a 0.5- μm uniform removal run on a 50-mm-diam part would require ~ 20 min. Lowest achieved rms roughness values were between 1 nm and 3 nm. Results for nanodiamonds were the highest (5 nm), and those for ZrO_2 were clearly the lowest (0.5 nm). As noted in the table, the CI used with ZrO_2 had a smaller median particle size than that used with the other abrasives, and this may have contributed in part to this excellent result. As also noted, all roughness results reported in the table for ZrO_2 were obtained with an 80- μm high-pass filter. Unfiltered data for the smoothest surfaces were 0.1 nm higher.

Table 96.III: Peak removal rates and lowest achieved rms roughness values for polymers with different abrasives in MRF.

Polishing Abrasive (vol % CI)	PMMA Acrylic		PS Dow Styrene	COP Zeonex		PC Lexan
	Puck	Coupon	Coupon	Puck	Coupon	Coupon
	[peak removal rate, $\mu\text{m}/\text{min}$] ^(d) lowest rms roughness (nm) ^(e)					
CeO_2 ^(a,b) (36)	[4.0] 1.6 \pm 0.1			[3.5] 1.9 \pm 0.7 ^(f)	1.45 \pm 0.06	
CeO_2 solution ^(c) (45)	[13.6]	3.9 \pm 1.1	157 \pm 27	[4.2]	13.3 \pm 9.5	3.6 \pm 0.7
Diamond ^(a,c) (45)	[3.7] 4.8 \pm 2.1		90 \pm 60	[2.6] 2.8 \pm 1.0	3.7 \pm 0.9	3.2 \pm 0.7
SnO_2 ^(b) (36)	[6.3] 1.4 \pm 0.4			[2.7] artifacts		
ZrO_2 ^(b,g) (36)	[3.6] 0.50 \pm 0.06 ^(h)	0.58 \pm 0.07 ^(h)	61 \pm 6 ^(h)	[0.8] 62 \pm 8 ^(h,i)	80 \pm 3 ^(h)	71 \pm 3 ^(h)
Al_2O_3 ^(c) (45)	[4.0] 1.5 \pm 0.1		6.1 \pm 0.2		4.1 \pm 0.9	3.1 \pm 0.7
TiO_2 ^(c) (45)	[14.6] 3.3 \pm 0.2 ⁽ⁱ⁾			[7.2] 6.9 \pm 2.0		
SiO_2 ^(c) (44)	[11.6] 2.8 \pm 0.2 ⁽ⁱ⁾			[4.6] 116 \pm 5 ⁽ⁱ⁾		
(a)standard MR fluid; (b)standard 150-mm-diam wheel; (c)small 50-mm-diam wheel; (d)standard dev. est. @ $\pm 2\%$, average of four spots; (e)after uniform $\sim 0.5\text{-}\mu\text{m}$ removal runs for PMMA and COP, amounts of material removed for PS and PC not determined due to lack of spot data; (f)0.2- μm removal run, measured in areas avoiding artifacts that appeared on surface; (g)smaller CI particles used in MR fluid; (h)80- μm high-pass filter; (i)inside a spot.						

PS: Coupons of this material were difficult to polish without increasing the surface roughness. Figure 96.39 shows the result of polishing with ZrO₂. Due to the evolution of surface artifacts rms roughness increased by nearly four times. Worse results were obtained for nanodiamonds. The best results were obtained with Al₂O₃. Initial areal p-v roughness of 1 μm was reduced to 56 nm, and the initial rms roughness of 6 nm was unchanged. No surface artifacts were generated.

COP: Under identical conditions, peak removal rates using most abrasives were two to four times lower than those measured for PMMA, except for the standard CeO₂-based and nanodiamond-based MR fluids. For these, removal rates were 13% (3.5 μm/min) and 30% (2.6 μm/min) lower, respectively. The removal rate for ZrO₂ (~0.8 μm/min) was too low to be practical, and there were other problems (see Fig. 96.39). Smoothing the surface without introducing artifacts was difficult. The values of rms roughness achieved with the standard CeO₂-based and nanodiamond-based MR fluids were lower (2 nm to 3 nm) than those measured with CeO₂ (solution), ZrO₂, TiO₂, or SiO₂, but significant numbers of surface artifacts were still generated. An artifact-free surface was obtained on a coupon using Al₂O₃, and the rms roughness was reduced from 9 nm (initial) to 4 nm (final).

PC: ZrO₂ degraded the coupon surface as seen in Fig. 96.39. Moderate numbers of artifacts developed after processing with the CeO₂ (solution) abrasive. The standard nanodiamond-based MR fluid was seen to reduce initial rms surface roughness from ~11 nm to ~3 nm. Similar results were observed for the Al₂O₃-based MR fluid (8 nm to 3 nm). The Al₂O₃-processed surface appeared to be the best.

2. Polishing COP (Zeonex) with the Standard CeO₂-Based MR Fluid

A 75-mm-diam by 25-mm-thick diamond-turned plano puck of COP (Zeonex) was processed on the Q22Y using the standard CeO₂-based MR fluid under gentle machine conditions. The spot removal rate was ~3.8 μm/min. Figure 96.40 shows areal roughness maps. The rms roughness (averaged over five sites) was reduced from ~23 nm to ~2 nm. Two figure-correction runs were also performed on the part. Over 90% of the aperture, p-v surface wavefront error was reduced from 1.53 μm to 0.39 μm. Inspection of the part after processing revealed a moderate number (~5/mm²) of artifacts on the part surface (see Fig. 96.41).

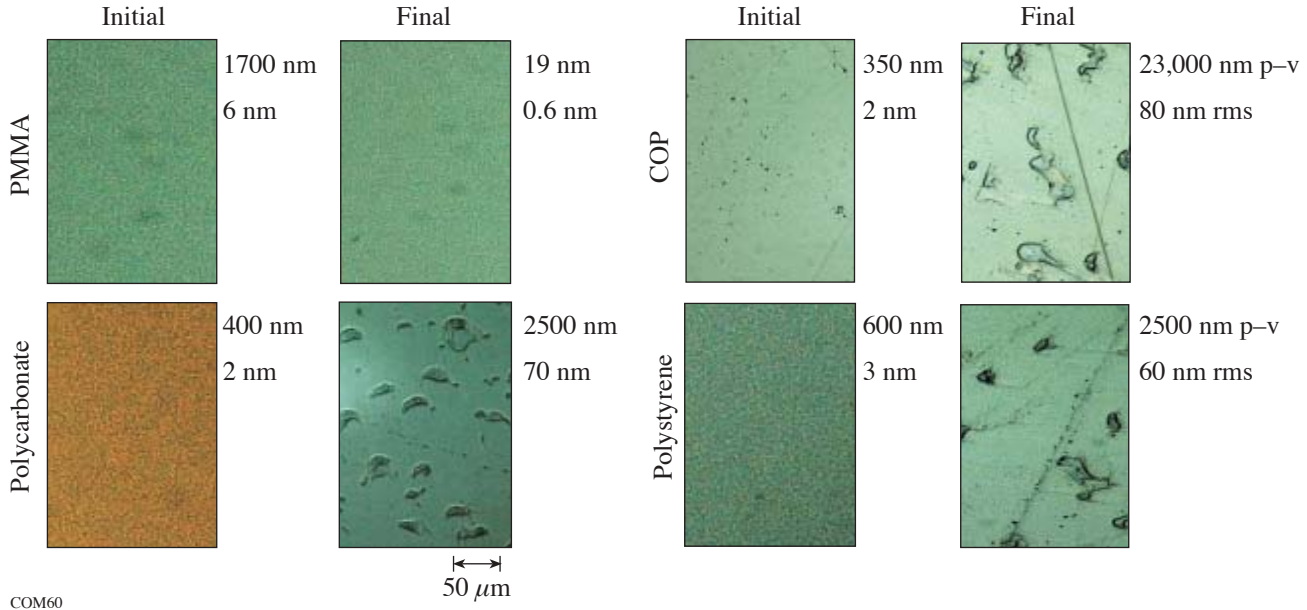


Figure 96.39 Optical microscopy of polymer surfaces after uniform 0.5-μm polishing runs with a ZrO₂-based MR fluid. Excellent results were observed for PMMA, but surface artifacts were created in PC, COP, and PS. Switching to an Al₂O₃-based MR fluid eliminated the artifact problem. (All photographs are to the scale indicated in the figure.)

3. Figure Correction and Removal of Diamond-Turning Marks on a PMMA Puck

Two 38-mm-diam by 7.8-mm-thick diamond-turned plano pucks of PMMA were processed in the Q22Y machine. One part was used to determine removal rates. White-light profilometry and laser interferometry were used to characterize one surface of the second puck for microroughness and figure (over 95% of the hard aperture) before and after each processing run. The backsides of these pucks were fine ground to simplify the metrology. Strategies were employed (described later) to minimize the time required for the pucks to come to thermal equilibrium prior to figure measurement. A ZrO₂-based MR fluid was used under standard machine conditions. This MR fluid showed excellent stability, and the experiment was conducted 9 days after the fluid had been loaded into the machine and used for other work.

The initial surface figure error of the diamond-turned PMMA puck was 4.45 μm p-v. The initial average microroughness values for this surface were 35±3 nm p-v and 3.8±0.3 nm rms. A power spectral density plot of the surface showed a strong peak at 300 lines per mm, indicating a 3-μm lateral diamond-turning groove spacing. Two figure correction runs were performed to bring down the figure error. The peak removal rate for run #1 was 3.62 μm/min and the run time was 170 min. The resulting figure error after run #1 was about 1.2 μm p-v. This value varied over time as the part recovered from the effects of handling, cleaning, and moving between the shop floor and the metrology lab. Placing the part between copper blocks in the metrology lab for 60 min and inserting padding between the part and the metal clamps in the interferometer mount helped to reduce thermal equilibration times, but ultimately the part was left in the metrology lab overnight.

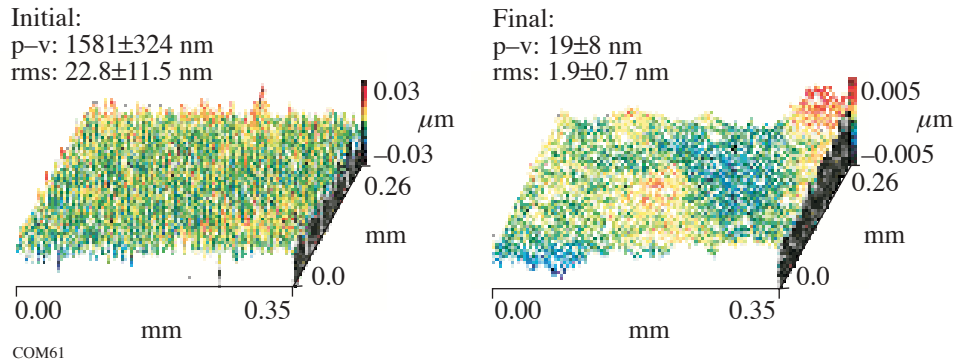


Figure 96.40

Example of areal roughness on COP surface before/after a 0.2-μm uniform removal run using a standard CeO₂-based MR fluid under “gentle” processing conditions. Numerical values given in the figure are averages of five sites.²²

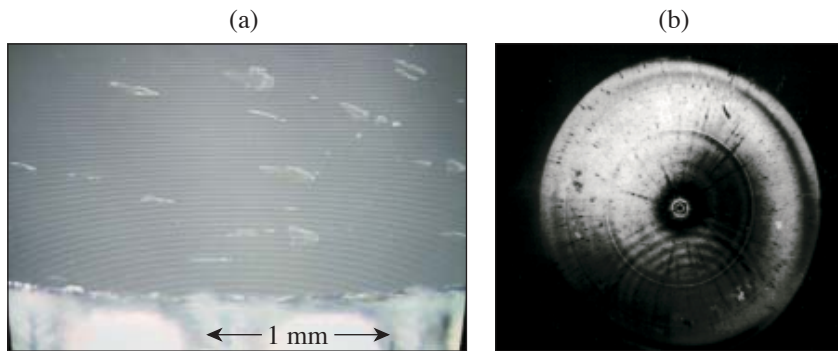
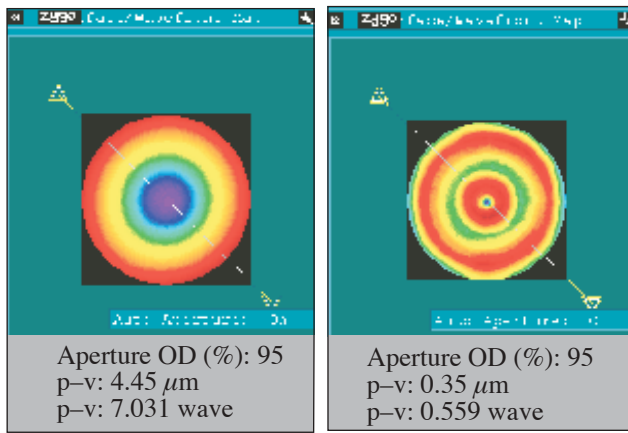


Figure 96.41

Artifacts in the surface of the COP puck at the conclusion of the polishing process: (a) view under microscope between crossed polarizers; (b) thermal printout of interferogram.

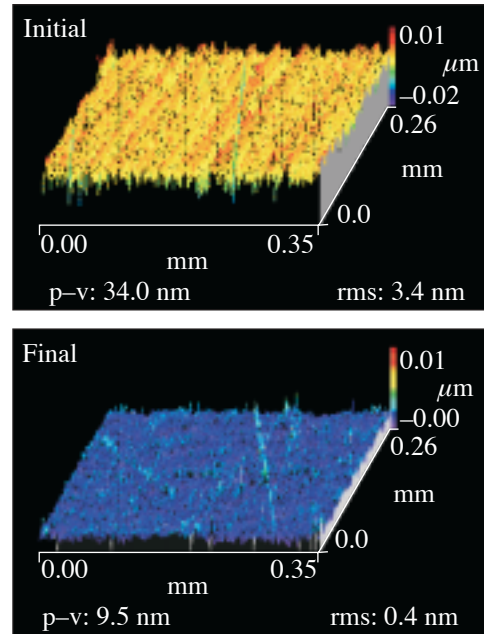
The peak removal rate for run #2 on day 2 was remeasured and found to be virtually unchanged at 3.63 $\mu\text{m}/\text{min}$. Upon completion of this second 40-min correction run, the figure error was further reduced from 1.2 μm p-v to ~ 0.35 μm p-v. Final surface microroughness values were 18.5 ± 6.8 nm p-v and 0.47 ± 0.05 nm rms. Power spectral density (PSD) plots confirmed that all diamond-turning marks had been eliminated. The PSD signature at 300 lines/mm was reduced in amplitude by over 1300 \times .



COM63

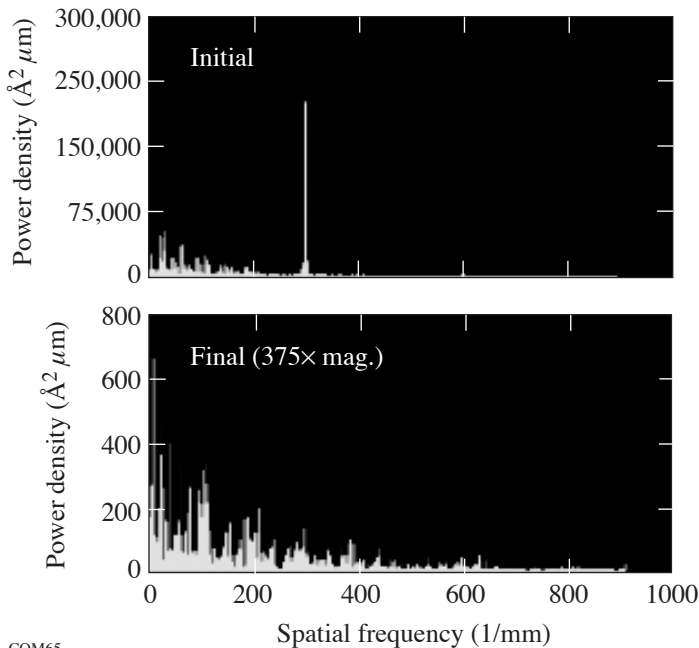
Figure 96.42 Initial and final wavefront maps for the PMMA puck (95% aperture).

Metrology results supporting the experimental findings are shown in Figs. 96.42 and 96.43. Figure 96.42 shows the initial and final wave-front maps for surface figure. Figure 96.43 shows initial and final oblique plots for surface roughness at a typical site, and Fig. 96.44 shows the initial and final power spectral density plots at the same site shown in Fig. 96.43.



COM64

Figure 96.43 Initial and final surface-roughness values for the PMMA puck at one typical site.



COM65

Figure 96.44 Initial and final PSD plots for the PMMA puck at the same site examined in Fig. 96.43. The diamond-turning mark signature at 300 lines/mm was reduced by more than 1300 \times . (The ordinate scale has been magnified by 375 \times to show the signature after MRF.)

4. Thermal Effects

Polymers require a longer time to thermalize than glasses, ceramics, or metals. This may be examined in two ways. The time ϕ (in minutes) required for a temperature gradient across the thickness t of a disk to decay to 10% of its initial value (heat being removed from only one side) is given as³⁴ $\phi = 1.67 \rho C_p t^2/k$, where ρ , C_p , and k are density, specific heat, and thermal conductivity, respectively. Table 96.IV gives a calculation of ϕ for 8-mm-thick pucks of PMMA and COP compared to the borosilicate glass BK7. The initial thermalization time for either of these polymers is four to five times longer than that for glass of equal thickness. Table 96.IV also gives a calculation of the sag S (in microns) of a part surface due to a linear temperature gradient through the thickness t as³⁴ $S = \alpha \Delta T r^2/2t$, where α , ΔT , and $2r$ are the coefficient of thermal expansion, the temperature difference across the part, and the part diameter (38 mm), respectively. A gradient of less than 0.2°C across a glass part is negligible, but for a polymer puck it is still sufficient to cause a 0.3- μm distortion.

Interferometry over 95% of its aperture was periodically performed on the 8-mm-thick PMMA puck used in the two figure correction runs previously described. The puck was “soaked” between two copper blocks for 30 min in the metrology lab and then monitored for p-v figure error after the first polishing run. Figure 96.45 shows that the initial figure error of 1.2 μm decayed to 1.0 μm after an additional 60 min. A similar measurement on the part at the conclusion of the second figure correction run showed that the same equilibration protocol was necessary to stabilize the surface figure at 0.4- μm p-v. Infrared thermometry³⁵ performed on the puck during polishing did not detect any rise in temperature above the ambient within the machine enclosure. This equilibration time is quite lengthy compared to the calculations shown above, suggesting that temperature fluctuations within the puck may

have been prolonged by the heavy traffic into and out of the metrology lab during the day. Precise interferometric testing is difficult to perform during the cold working of polymer optics.

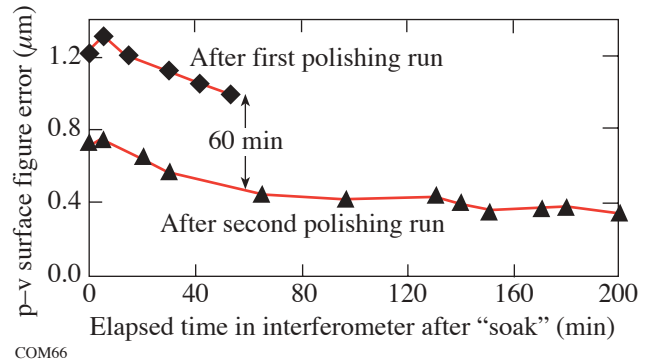


Figure 96.45 Wavefront metrology for an ~8-mm-thick PMMA puck as a function of elapsed time in the interferometer after a 30-min “soak” between copper plates. Stabilization required an additional 60 min (lines to guide the eye).

5. Long-Term Figure Instability in a PMMA Puck Polished on Both Sides

An experiment was conducted to polish out diamond-turned side 1 (S1) and side 2 (S2) of a plano PMMA puck. Puck dimensions and processing conditions were identical to those described above for the removal of diamond-turning marks. S1 was polished out on day 1 to a surface figure error of 0.33 μm p-v. S2 was polished out on day 2 to a surface figure error of 0.4 μm p-v. S1 was then monitored. Figure 96.46 shows the change in surface profile that was observed over 40 days. The center of the puck surface became concave, and by day 25 the surface figure error of S1 had degraded by almost 5 \times to 1.48 μm p-v. This had relaxed to 1.11 μm p-v by day 34, and to 1.09 μm p-v by day 40. We seek an explanation.

Table 96.IV: Thermal calculations for polymer and glass pucks 8 mm thick by 38 mm in diameter.

	Time to reduce temperature gradient across part to 10% of initial value					Sag in part surface from temperature gradient remaining across part (μm)			
	ρ (g/cc)	C_p (J/g°C)	t (cm)	k (W/m°C)	ϕ (min)	α (10^{-5} cm/cm°C)	$\Delta T = 5.0^\circ\text{C}$	$\Delta T = 1.0^\circ\text{C}$	$\Delta T = 0.2^\circ\text{C}$
Acrylic ^{14,36}	1.19	1.5	0.8	0.23	8	6.7	7.7	1.54	0.3
Zeonex ^{14,37}	1.01	1.35	0.8	0.14	10	6.5	7.5	1.50	0.3
BK-7 ³⁸	2.51	0.86	0.8	1.11	2	0.7	0.8	0.16	0.03

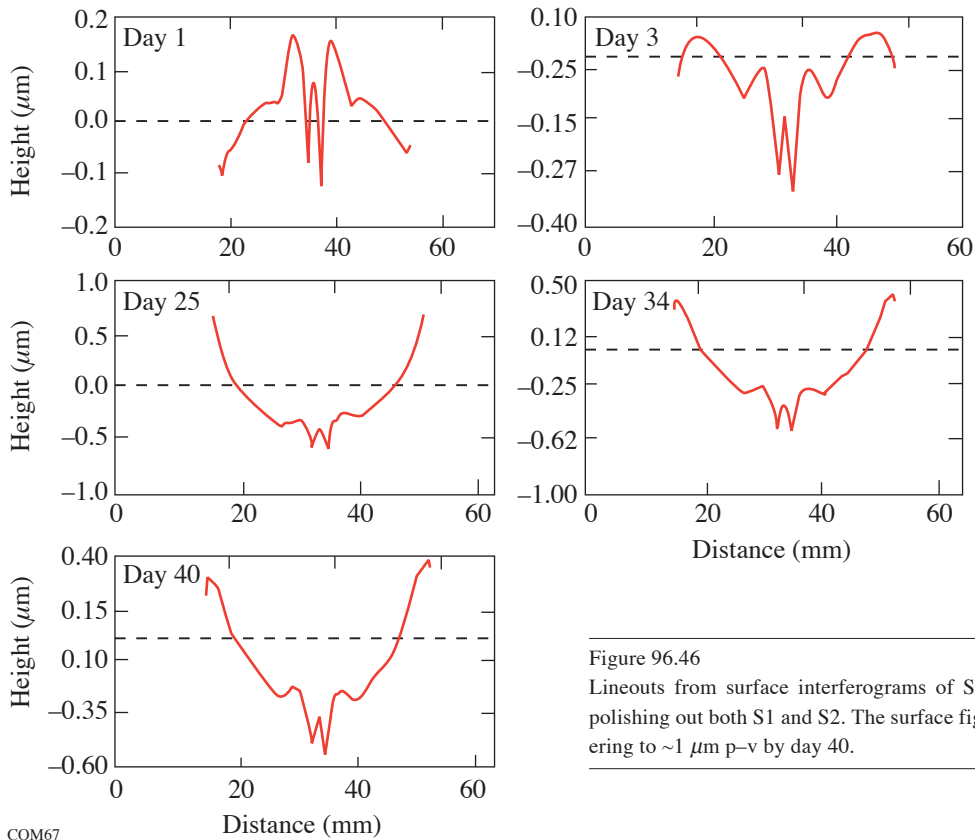


Figure 96.46

Lineouts from surface interferograms of S1 on a diamond-turned PMMA puck after polishing out both S1 and S2. The surface figure error degraded by 5 \times in 25 days, recovering to $\sim 1 \mu\text{m p-v}$ by day 40.

COM67

Conclusions

Experiments were conducted with conventional and experimental MR fluids to polish four optical polymers. A ZrO_2 -based MR fluid was successfully used on a Q22Y MRF machine to smooth and figure correct the plano surface of a diamond-turned PMMA part to 0.5 nm rms and 0.4 $\mu\text{m p-v}$, respectively. The diamond-turning marks were eliminated. Of the other abrasive/polymer combinations tested, Al_2O_3 showed the greatest potential for processing COP, PS, and PC without roughening or introducing surface artifacts. Issues of part thermalization for metrology were encountered. It was found that 90 min were required to stabilize the surface figure of an 8-mm-thick PMMA puck between runs and at the conclusion of a polishing experiment. Long-term surface figure instabilities were also observed for a PMMA puck after cold working both sides of the part.

ACKNOWLEDGMENT

Support for this work is provided by the Center for Optics Manufacturing. J. DeGroot is supported by the Frank J. Horton Graduate Fellowship Program.

REFERENCES

1. V. E. Sabinin and S. V. Solk, *J. Opt. Technol.* **69**, 48 (2002).
2. J. D. Lytle, "Polymetric Optics," in *Handbook of Optics*, 2nd ed., edited by M. Bass (McGraw-Hill, New York, 1995), Chap. 34, Vol. II, p. 34.13.
3. S. D. Jacobs, D. Golini, Y. Hsu, B. E. Puchebner, D. Stafford, Wm. I. Kordonski, I. V. Prokhorov, E. Fess, D. Pietrowski, and V. W. Kordonski, in *Optical Fabrication and Testing*, edited by T. Kasai (SPIE, Bellingham, WA, 1995), Vol. 2576, pp. 372–382.
4. D. Golini, S. Jacobs, W. Kordonski, and P. Dumas, in *Advanced Materials for Optics and Precision Structures*, edited by M. A. Ealey, R. A. Paquin, and T. B. Parsonage, *Critical Reviews of Optical Science and Technology* (SPIE, Bellingham, WA, 1997), Vol. CR67, pp. 251–274.
5. S. D. Jacobs, *Finer Points* **7**, 47 (1995).
6. S. R. Arrasmith, S. D. Jacobs, J. C. Lambropoulos, A. Maltsev, D. Golini, and W. I. Kordonski, in *Optical Manufacturing and Testing IV*, edited by H. P. Stahl (SPIE, Bellingham, WA, 2001), Vol. 4451, pp. 286–294.

7. I. Kozhinova, S. R. Arrasmith, J. C. Lambropoulos, S. D. Jacobs, and H. J. Romanofsky, in *Optical Manufacturing and Testing IV*, edited by H. P. Stahl (SPIE, Bellingham, WA, 2001), Vol. 4451, pp. 277–285.
8. J. D. Zuegel, V. Bagnoud, I. A. Begishev, M. J. Guardalben, J. Keegan, J. Puth, and L. J. Waxer, presented at CLEO, Baltimore, MD, 1–6 June 2003, invited paper CME3.
9. D. Golini *et al.*, *Laser Focus World* **37**, S5 (2001).
10. S. D. Jacobs, F. Yang, E. M. Fess, J. B. Feingold, B. E. Gillman, W. I. Kordonski, H. Edwards, and D. Golini, in *Optical Manufacturing and Testing II*, edited by H. P. Stahl (SPIE, Bellingham, WA, 1997), Vol. 3134, pp. 258–269.
11. S. R. Arrasmith, I. A. Kozhinova, L. L. Gregg, A. B. Shorey, H. J. Romanofsky, S. D. Jacobs, D. Golini, W. I. Kordonski, S. J. Hogan, and P. Dumas, in *Optical Manufacturing and Testing III*, edited by H. P. Stahl (SPIE, Bellingham, WA, 1999), Vol. 3782, pp. 92–100.
12. A. B. Shorey, S. D. Jacobs, W. I. Kordonski, and R. F. Gans, *Appl. Opt.* **40**, 20 (2001).
13. J. A. Menapace *et al.*, in *Laser-Induced Damage in Optical Materials: 2001*, edited by G. J. Exarhos *et al.* (SPIE, Bellingham, WA, 2002), Vol. 4679, pp. 56–68.
14. Data from *Specifications of Optical Grade Plastics*, G-S Plastic Optics, Rochester, NY 14603-1091.
15. Coupons were provided by Mr. William S. Beich, G-S Plastic Optics, Rochester, NY 14603-1091.
16. Diamond-turned pucks supplied by Mr. Paul Tolley, Syntec Technologies, Inc., Pavilion, NY 14525. Additional diamond turning of Zeonex pucks performed by Rochester Tool and Mold, Inc., Rochester NY 14611.
17. Extruded rod stock purchased from McMaster-Carr, New Brunswick, NJ 08903-0440; subsequently diamond turned by Rochester Tool and Mold, Inc., Rochester NY 14611.
18. This work was conducted by J. DeGroote and J. Watson as an independent laboratory experiment, in partial fulfillment of the requirements for the course Optics 256: Senior Lab, The Institute of Optics, University of Rochester, Rochester, NY, Fall 2001.
19. The permanent magnet machine was designed and fabricated for the Center for Optics Manufacturing in 1998 by Dr. I. Prokhorov and colleagues, Luikov Institute, Minsk, Belarus. It's capabilities and limitations are described in J. E. DeGroote, S. D. Jacobs, and J. M. Schoen, in *Optical Fabrication and Testing*, OSA Technical Digest (Optical Society of America, Washington, DC, 2000), pp. 6–9.
20. J. E. DeGroote, "Initial MRF Spotting Experiments on Optical Polymers," research project submitted in partial fulfillment of the requirements for Optics 443: Optical Fabrication and Testing, The Institute of Optics, University of Rochester, Rochester, NY, Spring 2002.
21. Q22, QED Technologies, LLC, Rochester, NY 14607.
22. Zygo NewView™ 5000 white-light optical profiler, Zygo Corporation, Middlefield, CT 06455. The instrument was set for areal mapping over 0.25 mm × 0.35 mm; 20× Mirau; FDA resolution: high; 20- μ m bipolar scan; min/mod: 5.
23. Zygo GPI xPHR phase-shifting laser interferometer, Zygo Corporation, Middlefield, CT 06455.
24. S. D. Jacobs, S. R. Arrasmith, I. A. Kozhinova, L. L. Gregg, A. B. Shorey, H. J. Romanofsky, D. Golini, W. I. Kordonski, P. Dumas, and S. Hogan, in *Finishing of Advanced Ceramics and Glasses*, edited by R. Sabia, V. A. Greenhut, and C. G. Pantano, Ceramic Transactions, Vol. 102 (The American Ceramic Society, Westerville, OH, 1999), pp. 185–199.
25. A. B. Shorey, S. D. Jacobs, W. I. Kordonski, and R. F. Gans, *Appl. Opt.* **40**, 20 (2001).
26. W. I. Kordonski and D. Golini, *J. Intell. Mater. Syst. Struct.* **10**, 683 (1999).
27. I. Kozhinova, S. Jacobs, S. Arrasmith, and L. Gregg, in *Optical Fabrication and Testing*, OSA Technical Digest (Optical Society of America, Washington, DC, 2000), pp. 151–153.
28. A. B. Shorey, K. M. Kwong, K. M. Johnson, and S. D. Jacobs, *Appl. Opt.* **39**, 5194 (2000).
29. Technical product literature, Universal Photonics, Inc., Hicksville, NY 11801-1014.
30. Technical product literature, Salem Distributing Company, Winston-Salem, NC 27103.
31. Technical product literature, Buehler Ltd., Lake Bluff, IL 60044-1699.
32. *Primary particle*: homogeneously ordered, single domain, single crystal; *aggregate*: two or more primary particles, strongly bonded together and difficult to separate; *agglomerate*: ensembles of primary particles or aggregates, loosely bonded together and easily separated. Definitions taken from "Fundamentals of Particle Sizing," Technical Notes (7/94) from Nanophase Technologies Corporation, Burr Ridge, IL 60521.
33. Horiba LA-900 Particle Size Analyzer, Horiba Instruments, Inc., Irvine, CA 92714.
34. F. Cooke, N. Brown, and E. Prochnow, *Opt. Eng.* **15**, 407 (1976).
35. Minitemp® IR thermometer from Raytek, Inc., Santa Cruz, CA 95061-1820.
36. G. W. C. Kaye and T. H. Laby, *Tables of Physical and Chemical Constants and Some Mathematical Functions*, 15th ed. (Longman, London, 1986), p. 289.
37. Data from product literature, Zeon Corporation, Tokyo, Japan 100-8323.
38. Data from *Optical Glass Catalog-1994*, Schott Glass Technologies, Inc., Duryea, PA 18642.

